Sensors and Materials, Vol. 31, No. 11 (2019) 3437–3449
MYU Tokyo

S & M 2022

Use of Extension Method with Chaotic Eye Features for Electrocardiogram Biometric Recognition

Mang-Hui Wang,[1] Mei-Ling Huang,[2*] Shiue-Der Lu,[1] and Zong-Yi Lee[1]

[1]Department of Electrical Engineering, National Chin-Yi University of Technology
57, Sec. 2, Chung Shan Rd., Taiping, Taichung 411, Taiwan, ROC
[2]Department of Industrial Engineering & Management, National Chin-Yi University of Technology,
57, Sec. 2, Chung Shan Rd., Taiping, Taichung 411, Taiwan, ROC

(Received April 23, 2019; accepted October 8, 2019)

Keywords: electrocardiogram (ECG), master–slave chaotic system, chaotic eyes, extension method, identity recognition, cardiac arrhythmia

An electrocardiogram (ECG) documents the voltage changes during heartbeats. It captures electrocardiographic signals in a noninvasive way. ECGs are complicated and vary from person to person, making them ideal for use in biometric recognition systems. A number of studies have shown that ECG signals are nonlinear curves and dynamically chaotic. The ECG signals were measured on the basis of the Einthoven's triangle principle in this study. Combining captured ECG signals using ECG biosensors and a data acquisition (DAQ) card, LabVIEW was used to design a human–machine interface (HMI) to display the processed ECG signals for test subjects. The saved ECG data were plotted in a dynamical map of the chaotic dynamic error using a master–slave chaotic system. The chaotic eye was selected as a feature and an identity database was built using an element model. Personal identity was identified by categorizing with an extension method. Thirty-six subjects were tested and the identification accuracy was 94.4%. The MIT-BIH Normal Sinus Rhythm Database (NSRDB) and an arrhythmia database were used in this study. Using the extension method, the classification accuracy between normal and cardiac arrhythmia was 91.67%, and the accuracy was increased to 100% when matter element extensibility was employed. Results suggested that the biometric recognition method developed in this study performs identification rapidly with high positive recognition rate and reliability.

1. Introduction

Advanced modern technology and the availability of information have triggered the increasing use of network activities such as e-business curfew control, data access, and online transactions. With this technology, the application and development of identity recognition and security verification have become key issues.(1) Traditionally, biometric recognition technology relies on body and behavioral features. The former requires meticulous identification because unique body features are captured for identification. The latter requires convenience of

*Corresponding author: e-mail: huangml@ncut.edu.tw
https://doi.org/10.18494/SAM.2019.2478

ISSN 0914-4935

identification because differences in human behaviors are used for identification.[2] The traditional biometric recognition techniques available are identification by facial recognition, fingerprint, voice, eyeball, and DNA.[3–5] However, these techniques come with certain limitations. A novel biometric recognition method is expected to resolve and improve the limitations and drawbacks of the traditional ways.

Electrocardiogram (ECG) signals are complicated and differ from person to person, and are therefore difficult to duplicate or steal, making them applicable to biometric recognition. ECG signals have been studied extensively and used in clinical applications for many years.[6] In recent years, studies have shown that ECG signals captured through ECG biosensors can be used for the biometric recognition and assessment of heart health to further monitor or prevent the occurrence of heart diseases.[7–11]

The time domain, frequency domain, wavelet analysis, and hybrid algorithms are common feature selection methods used in ECG identification in related studies. For example, the PQRST waves were measured on ECG detection via the time domain. The QRS complex wave and intervals were featured for ECG recognition, and the major classification methods included neural networks,[12,13] linear discriminant analysis,[14,15] support vector machine,[16] the two-pass classification method,[17] and fuzzy theory.[18] Although hybrid classification methods combining the above-mentioned multiple classification methods enhance the recognition accuracy, because of the computational complexity, more execution time is required in the training phase.

A number of studies have found that ECG signals are nonlinear curves and dynamically chaotic.[19–21] On this basis, in this study, a master–slave chaotic ECG dynamic error system was proposed to capture the chaotic eye as a feature, and the extension method was used for classification to identify personal identity and cardiac arrhythmia.

2. Materials and Methods

The proposed ECG biometric recognition system consists of three functions: ECG signal capturing and preprocessing, feature extraction, and identity recognition. First, the ECG signals are captured by a hardware circuit, a data acquisition (DAQ) card, and LabVIEW, and then converted to a dynamical map of the chaotic dynamic error using a master–slave chaotic system to find the coordinates of the chaotic eye, which serves as the feature for an element model to be found in an identity recognition database. Next, the extension method is used for classification. Finally, there is a human–machine interface (HMI) whose design was based on LabVIEW. Figure 1 shows a flowchart of this study.

2.1 ECG signal capture and preprocessing

The ECG capturing circuit comprised electrode patches, a preamplifier, a filter, and an amplifier. Figure 2 shows the process followed to capture ECG signals.

The electrode patches were attached in Einthoven's triangle. The principle behind this is to divide the standard bipolar limb lead into three leads: Leads I, II, and III. Lead I measures the

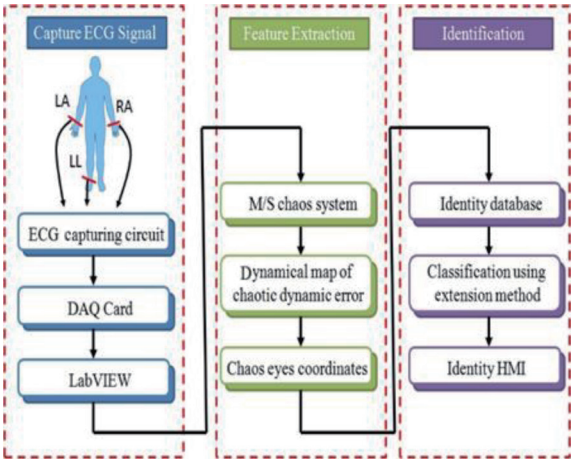

Fig. 1. (Color online) System flowchart.

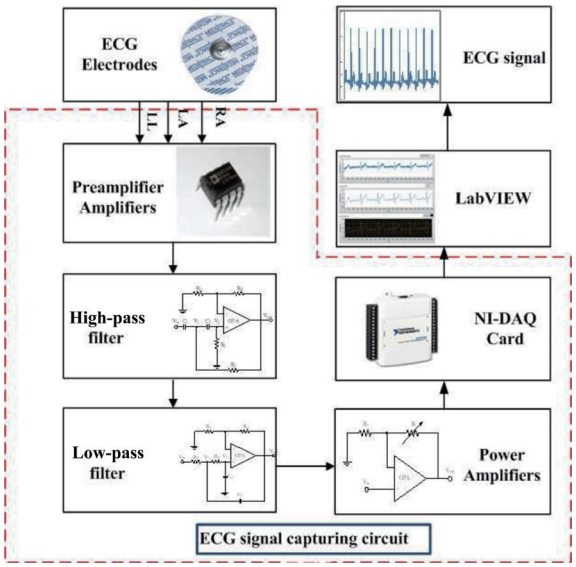

Fig. 2. (Color online) ECG signal capturing process.

difference in potential between the left hand (LA) (positive) and the right hand (RA) (negative) with 0° orientation; Lead II measures the difference in potential between the left leg (LL) (positive) and the right hand (RA) (negative) (II = LL – RA) with 60° orientation; and Lead III measures the difference in potential between the left leg (LL) (positive) and the left hand (LA) (positive) (III = LL – LA) with 120° orientation. Because II = I + III, the Einthoven triangle is complete.

An AD620 amplifier was used as the preamplifier, which is a high-gain and DC coupling amplifier, and features a differential input, a single-end output, a high input impedance, and a high common mode rejection ratio. The filters were a second-order Butterworth low-pass filter and a second-order Butterworth high-pass filter, as shown in Figs. 3 and 4, respectively. These were designed to keep the ECG signals within 0.05 and 100 Hz, respectively.[22]

The signals were captured by the circuit and DAQ card through the electrode patches and converted them into ECGs using LabVIEW. The ECG data were saved for a minute after they were measured from the test subject. Figure 5 shows the ECG HMI of a test subject generated by LabVIEW.

2.2 Feature extraction

The features of the test subject's ECG were extracted using a chaotic system. In the chaotic system, the minute changes in ECG signals lead to huge variations as time evolves. The chaotic dynamic error system extracts the dynamic errors between two chaotic systems by adding and subtracting them.[23] The original measured ECG signals are transformed to chaotic dynamic error scatter plots through chaotic theory. Each chaotic scatter plot has two chaotic eyes, and the coordinates of the two eyes are used as features for further processing in the extension method.

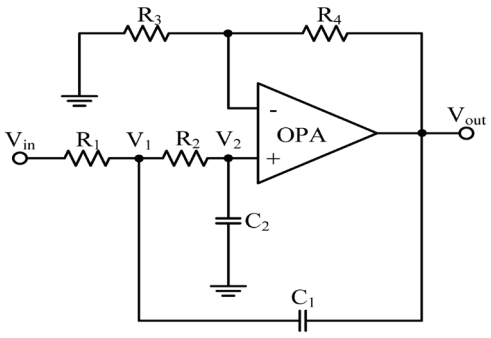

Fig. 3. Second-order Butterworth low-pass filter.

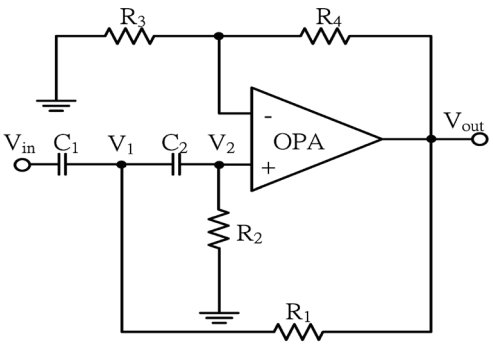

Fig. 4. Second-order Butterworth high-pass filter.

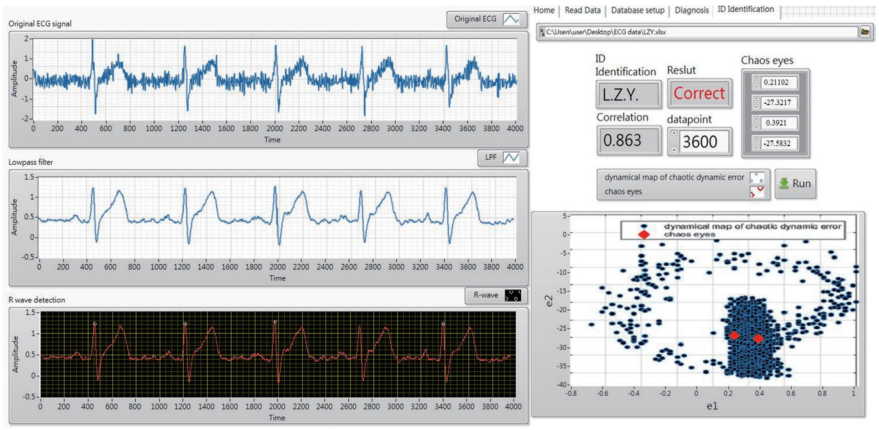

Fig. 5. (Color online) ECG HMI of test subject generated by LabVIEW.

The master (S_{master}) and slave (S_{slave}) of a master–slave system are expressed by Eqs. (1) and (2), respectively.

$$S_{master} = \begin{cases} \dot{x}_1 = f_1(x_1, x_2, ..., x_n) \\ \dot{x}_2 = f_2(x_1, x_2, ..., x_n) \\ \quad \vdots \\ \dot{x}_n = f_n(x_1, x_2, ..., x_n) \end{cases} \tag{1}$$

$$S_{slave} = \begin{cases} \dot{y}_1 = f_1(y_1, y_2, ..., y_n) \\ \dot{y}_2 = f_2(y_1, y_2, ..., y_n) \\ \quad \vdots \\ \dot{y}_n = f_n(y_1, y_2, ..., y_n) \end{cases} \tag{2}$$

Here, f_i (=1, 2, ..., n) is a nonlinear function. By subtracting Eq. (2) from Eq. (1), the master and slave dynamic error is generated, as expressed in Eq. (3). A calculation yields the chaotic dynamic function as Eq. (4).

$$\begin{cases} e_1 = x_1 - y_1 \\ e_2 = x_1 - y_2 \\ \quad \vdots \\ e_n = x_n - y_n \end{cases} \tag{3}$$

$$\begin{cases} \dot{e}_1 = f_1(x_1, x_2, ..., x_n) - f_1(y_1, y_2, ..., y_n) \\ \dot{e}_2 = f_2(x_1, x_2, ..., x_n) - f_2(y_1, y_2, ..., y_n) \\ \quad \vdots \\ \dot{e}_n = f_n(x_1, x_2, ..., x_n) - f_n(y_1, y_2, ..., y_n) \end{cases} \tag{4}$$

The Lorenz chaotic system is employed in this study. The master (L_{master}) and slave (L_{slave}) Lorenz systems are expressed by Eqs. (5) and (6), respectively.

$$L_{master} = \begin{cases} \dot{x}_1 = \alpha(x_2 - x_1) \\ \dot{x}_2 = \beta x_1 - x_1 x_3 - x_2 \\ \dot{x}_3 = x_1 x_2 - \gamma x_3 \end{cases} \tag{5}$$

$$L_{slave} = \begin{cases} \dot{y}_1 = \alpha(y_2 - y_1) \\ \dot{y}_2 = \beta y_1 - y_1 y_3 - y_2 \\ \dot{y}_3 = y_1 y_2 - \gamma y_3 \end{cases} \tag{6}$$

By subtracting Eq. (6) from Eq. (5), the chaotic dynamic function of the Lorenz master–slave system is obtained in the matrix form as[24]

$$\begin{bmatrix} \dot{e}_1 \\ \dot{e}_2 \\ \dot{e}_3 \end{bmatrix} = \begin{bmatrix} -\alpha & \alpha & 0 \\ \beta & -1 & 0 \\ 0 & 0 & -\gamma \end{bmatrix} \begin{bmatrix} e_1 \\ e_2 \\ e_3 \end{bmatrix} + \begin{bmatrix} y_2 y_3 - x_2 x_3 \\ -y_1 y_3 + x_1 x_3 \\ y_1 y_2 - x_1 x_2 \end{bmatrix}, \tag{7}$$

where x is the master system with an initial value of zero, y is the slave system containing ECG signal values, α, β, and γ are the adjusted error coefficients that are based on Lorenz's experience values, which are set as 10, 28, and −3/8, respectively, and e_1 and e_2 are used to generate the dynamical map of the chaotic dynamic error. The coordinates of the two centers of gravity in the map are defined as the chaotic eyes and used as features in the biometric recognition system.[25]

2.3 Recognition method

The ECG signals are processed by the chaotic system to yield the features of the chaotic eyes before the extension method is used for classification. The mathematical methods of the extension set and correlation function are practical tools for extension evaluation. For

extension evaluation, multiple databases are established through experiments. A single object is decomposed into one or more level sets and an expert system defines the range for these level sets. The data of the object to be evaluated are substituted into the data range of these level sets for extension correlation and normalization. The results of the calculation are compared with the extension correlation of each of these sets. The closer the extension correlation is to 1, the better the data of the object to be evaluated fit the specific set. The following are the steps of the biometric recognition.[26]

Step 1: Build an element model and define the classic domain as in Eq. (8). The theory is that an object R is divided into k levels of numeric sets. This is the classic domain of each of the sets. Therefore, a database has to be built before identity recognition.

$$R_k = (N_k, C_i, X_{ki}) = \begin{bmatrix} N_k & C_1 & < a_{k1}, b_{k1} > \\ & C_2 & < a_{k2}, b_{k2} > \\ & \vdots & \vdots \\ & C_n & < a_{kn}, b_{kn} > \end{bmatrix} \tag{8}$$

Here, N_k is the name of the element in each of the k levels of sets, C_i is the feature of the element name expressed as C_i (i = 1 – n), X_{ki} means that this feature range falls in the distribution range of the ith feature of the kth level, a_{ki} is the magnitude of this feature, a_{ki} (i = 1 – n) is the maximum of the element level set feature, b_{ki} is the magnitude of this feature, and b_{ki} (i = 1 – n) is the minimum of the element level set feature.

Step 2: Determine the test element. An unknown element is divided into the features of each level of sets. The number of levels of sets equals that of classic and joint domains combined. This is called the element to be tested, which is expressed as

$$R = (q, C_i, X_i) = \begin{bmatrix} q & c_1 & x_1 \\ & c_2 & x_2 \\ & \vdots & \vdots \\ & c_n & x_n \end{bmatrix}, \tag{9}$$

where q is the name of the ECG test subject and x_i is the chaotic eye feature data of c_i (i = 1, 2, 3, 4).

Step 3: Provide weights for the features. The object R consists of features c_i. Each of the features has an effect on the object. The correlation of the weight coefficient is used in this step to determine the weight percentage of each feature contributing to the object, as shown by

$$\sum_{i=1}^{4} W_i = 1. \tag{10}$$

Step 4: The correlation between the data to be measured and each category is determined. This refers to the distance between a feature of an element to be tested, x_i, and the center of that

element in all of the classic or joint domains. This distance is defined as the range, as shown in Eq. (11), and it is the same for the feature range in the joint domain.

$$\rho\left(x_i, X_{ki}\right) = \left| x_i - \frac{a_{ki} + b_{ki}}{2} \right| - \frac{b_{ki} - a_{ki}}{2} \tag{11}$$

Step 5: Calculate the correlation function. If the classic and joint domain ranges are determined, the correlation function is solved by using Eq. (12), i.e., to determine the degree of correlation. Then, the summation in Eq. (13) is carried out to obtain the correlation of the object to be tested. The category which the object falls into is clearly identified.

$$k_k(x_i) = \begin{cases} \dfrac{-\rho(x_i, X_{ki})}{\left|X_{ki}\right|}, & x_i \in X_{ki} \\ \dfrac{\rho(x_i, X_{ki})}{\rho(x_i, X_{pi}) - \rho(x_i, X_{ki})}, & x_i \notin X_{ki} \end{cases} \tag{12}$$

$$k_k(q) = \sum_{i=1}^{n} W_i k_k(x_i) \tag{13}$$

Step 6: Normalize the correlation. By determining the relative values of the correlation to each of the sets, the normalization is performed using Eq. (14) to allow the correlation to fall between −1 and 1.

$$\overline{k}_{k(q)} = \frac{2k_{k(q)} - k_{k(q)max} - k_{k(q)min}}{k_{k(q)max} - k_{k(q)min}} \tag{14}$$

Step 7: Evaluate the identity of the element. When $k_{k(q)}$ is equal to 1, the correlation is category k. The possibility of other set patterns depends on the correlation. In general, the greater the correlation for a specific set, the more likely the element being evaluated is close to that specific set. The diagnosis ends when all the elements are evaluated. Otherwise, evaluate new elements by going back to Step 2.

3. Experimental Results

The ECG capturing circuit and the DAQ card proposed in this study are shown in Fig. 6. The ECG signals were processed by LabVIEW and the processed ECG data were saved.

The master–slave system is used to generate the dynamical tracks and a map of the chaotic dynamic error. The values of the chaotic eyes are captured as the features for identity recognition. The chaotic eye is the center of gravity of the dynamical map of the chaotic dynamic error. Therefore, each test subject should have four features (c_1–c_4), as shown in Fig. 7, where c_1 is the value of the left chaotic eye on the X-axis (e_1), c_2 is the value of the left chaotic

Fig. 6. (Color online) ECG signal capturing circuit.

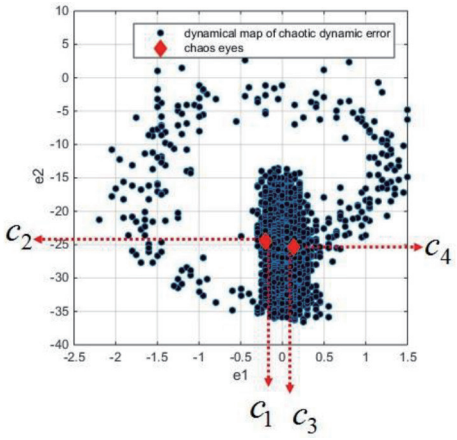

Fig. 7. (Color online) Definition of chaotic eyes.

eye on the *Y*-axis (e_2), c_3 is the value of the right chaotic eye on the *X*-axis, and c_4 is the value of the right chaotic eye on the *Y*-axis.

3.1 Personal identity recognition

To demonstrate the performance of the proposed method, 36 subjects with a healthy heart rate (23 males and 13 females), aged between 20 and 50, were tested. Half of the test samples were selected from the MIT-BIH Normal Sinus Rhythm Database (NSRDB).[27] Each subject underwent five tests (the total number of tests was 180). The recognition database contains five heart rates and chaotic eyes for each subject. The loci of the chaotic dynamic error for two subjects are shown in Figs. 8(a) and 9(a), and the corresponding dynamic maps of the chaotic dynamic error and chaotic eyes are plotted in Figs. 8(b) and 9(b), respectively. The data used in Fig. 8 were from a test subject, and those used in Fig. 9 were from the MIT-BIH NSRDB. Comparing the plots in Figs. 8 and 9, it is clear that the loci, dynamic maps, and chaotic eyes from different subjects have different natures. The results show that 170 out of the 180 tests produced positive recognition with an average recognition rate of 94.4% at an average time of 2.07. The proposed method was compared with other methods in terms of accuracy, as shown in Table 1.

3.2 Diagnosis of cardiac arrhythmia

In this section, normal sinus rhythm samples from the MIT-BIH normal database (NSRDB 16265, 16272, 16273, 16420, 16483) and arrhythmia samples from the MIT-BIH arrhythmia database (MITDB 109, 111, 214, 118, 124, 220, 223) were used. The left and right chaotic eyes C2 and C4 were identified as the features, and the weights were set as 0.5 for both features. The arrhythmia database used in this study includes types of normal sinus rhythm, left bundle branch block (LBBB), right bundle branch block (RBBB), and atrial premature contraction (APC).

The signals were sampled every 10 over a duration of 1 min for each subject. There were six samples for each subject. The first three samples were used as training sets and the last

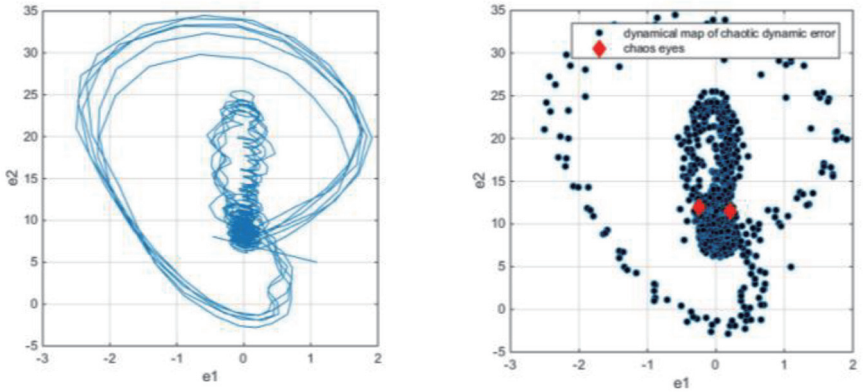

(a) (b)

Fig. 8. (Color online) (a) Locus of chaotic dynamic error from one test subject and (b) dynamic map of chaotic dynamic error and chaotic eye from the same test subject.

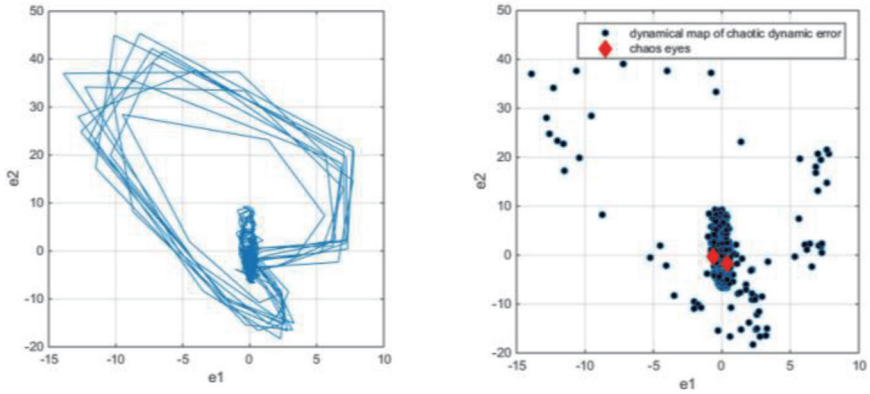

(a) (b)

Fig. 9. (Color online) (a) Locus of chaotic dynamic error from one MIT-BIH subject and (b) dynamic map of chaotic dynamic error and chaotic eye from the same MIT-BIH subject.

Table 1
Comparison with different methods.

Authors	Data source	Methods	Accuracy (%)
Wang *et al.*[28]	PTB database	PCA + LDA	≥90
Plataniotis *et al.*[29]	PTB database	AC + DCT	92.8
Chen *et al.*[30]	MIT-BIH	Neural network	75–90
Chan *et al.*[31]	Collected from lab	Wavelet distance	89
Loong *et al.*[32]	Collected from lab	LPC + WPD	≥90
Chen *et al.*[33]	Collected from lab	Chaotic theory + BPNN	91
Proposed method	MIT-BIH and collected from lab	Chaotic eye features + extension method	94.4

three samples were treated as testing sets. There were 36 training and 36 testing records in total. The values of the left chaotic eye on the *Y*-axis (e_2) and the right chaotic eye on the *Y*-axis (e_4) represent the classification features in Fig. 10(a). The four types of ECG beats are marked according to the classical domains for each type. As presented in Fig. 10(a), some

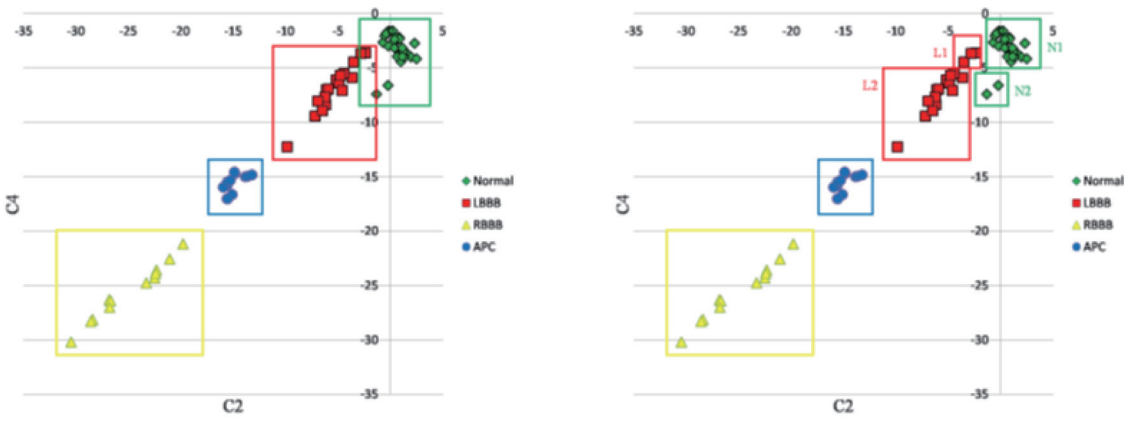

(a) (b)

Fig. 10. (Color online) (a) Plot of four types of beats based on extension method and (b) plot of four types of beats based on extension method and matter element extensibility.

Table 2
Comparison with different methods.

Authors	Data source	Methods	Accuracy (%)
Acharya *et al.*[34]	MIT-BIH	FFNN + fuzzy	≥90
Nasiri *et al.*[35]	MIT-BIH	SVM	92.8
Tang and Shu[36]	MIT-BIH	Gradient descent method	75–90
Jadhav *et al.*[37]	UCI	Multilayer Perceptron Neural Network	89
Proposed method	MIT-BIH	Chaotic eye features + extension method[38]	91.67
		Matter element extensibility	100

overlap occurring between the normal and LBBB types caused misclassification. Thirty-three out of the 36 subjects were classified correctly. The proposed method thus achieved an overall accuracy of 91.67%.

To enhance the accuracy, matter element extensibility was applied to separate the overlapping between the normal and LBBB types. The normal type was split into N1 and N2 and the LBBB type was split into L1 and L2 in Fig. 10(b). There was no overlap between the normal and LBBB types and an accuracy of 100% was achieved. To demonstrate the performance of the proposed method, a comparison with other related methods is given in Table 2. The 100% accuracy of the proposed extension method with matter element extensibility exceeded the performance of all other methods.

4. Conclusions

Using ECG signals captured through ECG biosensors and a DAQ card, we designed a HMI to display and save processed ECG signals for test subjects via LabVIEW. Using the proposed feature selection method proposed in this study, the dynamical map of chaotic dynamic error was plotted and the chaotic eye was selected as the feature. An element model was used to build an identity database and an extension method was applied to recognize personal identity and cardiac arrhythmia. Thirty-six subjects were tested and the identification accuracy was

94.4%. The MIT-BIH NSRDB and an arrhythmia database were used in this study. Using the extension method, the classification accuracy between normal and cardiac arrhythmia was 91.67%, and the accuracy was increased to 100% when matter element extensibility was employed. Compared with the other methods, the proposed method has fewer selected features of the ECG dataset in the time and frequency domains and markedly decreases the computing time and system complexity. Our results suggest that the identity recognition method developed in this study achieves rapid identification and has a high positive recognition rate.

References

1 J. Shen, S. D. Bao, L. C. Yang, and Y. Li: 2011 Annual Int. Conf. IEEE Engineering in Medicine and Biology Society (IEEE, 2011) 5248.
2 J. Ortega, J. Bigun, and D. Reynolds: IEEE Signal Process. Mag. **21** (2004) 2.
3 J. Tian and Y. Peng: 2012 Image Analysis and Signal Processing (IASP, 2012) 1.
4 V. G. Garagad and N. C. Iyer: 2014 Advances in Computing, Communications and Informatics (ICACCI, 2014) 973.
5 W. R. Schwartz, H. Guo, J. Choi, and L. S. Davis: IEEE Trans. Image Process. **21** (2012) 4.
6 C. Ye, M. T. Coimbra, and B. V. K. Vijaya Kumar: 2010 Annual Int. Conf. IEEE Engineering in Medicine and Biology (IEEE, 2010) 1918.
7 R. Palaniappan and S. Krishnan: 2004 Int. Conf. Signal Processing and Communications (ICSPCS, 2004) 569.
8 M. Sansone, R. Fusco, A. Pepino, and C. Sansone: J. Healthcare Eng. **4** (2013) 4.
9 A. Fratini, M. Sansone, P. Bifulco, and M. Cesarelli: Biomed. Eng. Online **14** (2015) 1.
10 M. Merone, P. Soda, M. Sansone, and C. Sansone: Expert Syst. Appl. **67** (2017) 189.
11 I. Odinaka, P. H. Lai, A. D. Kaplan, J. A. O'Sullivan, E. J. Sirevaag, and J. W. Rohrbaugh: IEEE Trans. Inf. Forensics Secur. **7** (2012) 6.
12 Z. Dokur and T. Olmez: Comput. Methods Programs Biomed. **66** (2001) 66.
13 J. Pardey: 2006 Computers in Cardiology (CinC, 2006) 485.
14 P. de Chazal, M. O'Dwyer, and R. Reilly: IEEE Trans. Biomed. Eng. **51** (2004) 7.
15 M. Llamedo and J. P. Martinez: IEEE Trans. Biomed. Eng. **58** (2011) 3.
16 K. Park, B. Cho, D. Lee, S. Song, J. Lee, Y. Chee, I. Kim, and S. Kim: 2008 Computers in Cardiology (CinC, 2008) 229.
17 M. Llamedo and J. P. Martinez: 2007 Computers in Cardiology (CinC, 2017) 105.
18 R. Silipo, W. Zong, and M. Berthold: Computers in Cardiology 1999 (CinC, 1999) 679.
19 S. C. Fang and H. L. Chan: Pattern Recognit. **42** (2009) 9.
20 R. B. Govindan, K. Narayanan, and M. S. Gopinathan: Chaos **8** (1998) 2.
21 H. Kantz and T. Schreiber: Inst. Elec. Eng. Proc. Sci. Meas. Technol. **145** (1998) 6.
22 M. H. Wang and Y. T. Su: Expert Syst. Appl. **39** (2012) 17.
23 H. J. C. Huijberts, H. Nijmeijer, and R. M. A. Willems: IEEE Trans. Circuits Syst. I, Fundam. Theory Appl. **47** (2000) 6.
24 C. H. Huang, C. H. Lin, and C. L. Kuo: IEEE Trans. Power Delivery **26** (2010) 2.
25 H. T. Yau and M. H. Wang: IET Renewable Power Gener. **9** (2015) 6.
26 M. H. Wang, H. T. Yau, and T. Y. Wang: Abstr. Appl. Anal. **2013** (2013) 8.
27 MIT-BIH Database.
28 Y. Wang, K. N. Plataniotis, and D. Hatzinakos: 2006 Biometrics Symposium: Special Session on Research at the Biometric Consortium Conference (BYSM, 2006) 1. Aug. 2006.
29 K. N. Plataniotis, D. Hatzinaos, and J. K. M. Lee: 2006 Biometrics Symposium: Special Session on Research at the Biometric Consortium Conference (BCC, 2006) 1.
30 H. Chen, K. K. Tseng, F. Zeng, H. N. Huang, and S. Y. Tu: 2012 12th Int. Conf. Hybrid Intelligent Systems (HIS, 2012) 427.
31 A. D. C. Chan, M. M. Hamdy, A. Badre, and V. Badee: IEEE Trans. Instrum. Meas. **57** (2008) 2.
32 J. L. C. Loong, K. S. Subari, R. Besar, and M. K. Abdullah: World Acad. Sci. Eng. Technol. **68** (2010) 44.
33 C. K. Chen, C. L. Lin, S. L. Lin, Y. M. Chiu, and C. T. Chiang: IEEE Comput. Intell. Mag. **9** (2014) 1.
34 R. Acharya, A. Kumar, P. S. Bhat, C. M. Lim, S. S. lyengar, N. Kannathal, and S. M. Krishnan: Med. Biol. Eng. Comput. **42** (2004) 3.

35 J. A. Nasiri, M. Naghibzadeh, H. S. Yazdi, and B. Naghibzadeh: Comput. Model: Simul. (2009) 187.
36 X. Tang and L. Shu: Multimedia Ubiquitous Eng. **9** (2014) 2.
37 S. M. Jadhav, S. L. Nalbalwar, and A. A. Ghatol: Int. J. Comput. Appl. **44** (2012) 15.
38 M. H. Wang and Z. Y. Lee.: 2016 IEEE 14th Int. Conf. IEEE (IEEE, 2016).

About the Authors

Meng-Hui Wang received his M.S. degree in electrical engineering (1990) and his Ph.D. degree in the same field (1994) from National Taiwan University of Science and Technology. He came to National Chin-Yi University of Technology (NCUT) in August 1994 and is now affiliated with the Department of Electrical Engineering as a distinguished professor. His major areas of research include renewable energy systems, power systems, extension theory, and AI applications. He is a member of the Chinese Association of Artificial Intelligence (CAAI), the Vice President of the Taiwan Education Society of Innovation & Invention (TESII), and also an Executive Committee Member of the Intelligent Living Technology Association of Taiwan (ILTAT). He was the General Chair of the 1st Intelligent Living Technology Conference (2006) and the Honorary Co-Chair of the 2012 International Symposium on Computer, Consumer and Control (IS3C). (wangmh@ncut.edu.tw)

Mei-Ling Huang received her M.S. and Ph.D. degrees in industrial engineering from University of Wisconsin–Madison and National Chiao-Tung University, respectively. Now, she is affiliated with the Department of Industrial Engineering and Management at National Chin-Yi University of Technology. Her research interests include quality management, quality engineering, data mining, and medical diagnosis. (huangml@ncut.edu.tw)

Shiue-Der Lu received his M.S. degree from Chung Yuan Christian University, Taoyuan City, Taiwan, in 2006, and his Ph.D. degree from the National Taiwan University of Science and Technology, Taipei City, Taiwan, in 2013, both in electrical engineering. From 2012 to 2016, he was a researcher at the Industrial Technology Research Institute. From 2016 to 2018, he was an assistant researcher at the Department of Electrical Engineering, Chung Yuan Christian University. Since 2018, he has been with the Department of Electrical Engineering, National Chin-Yi University of Technology, Taichung City, Taiwan, where he is currently an assistant professor. His research interests include renewable energy, power quality, damage diagnosis of wind power generators, and artificial intelligence applications in power systems. (sdl@ncut.edu.tw)

Zong-Yi Lee received his B.S. and M.S. degrees from the Department of Electrical Engineering, National Chin-Yi University of Technology, Taichung City, Taiwan, in 2015 and 2017, respectively. His research interests are in artificial engineering and bioengineering. (leezyi12345@gmail.com)